Tiago J. C. Sousa, Vítor Monteiro, J. G. Pinto, José A. Afonso, João L. Afonso

"Unified Architecture of Single-Phase Active Power Filter with Battery Interface for UPS Operation"

http://www.iaeng.org/publication/WCE2017/WCE2017_pp357-362.pdf

Unified Architecture of Single-Phase Active Power Filter with Battery Interface for UPS Operation

Tiago J. C. Sousa, Vítor Monteiro, J. G. Pinto, José A. Afonso, *Member, IAENG*, and João L. Afonso

Abstract—**This paper presents a shunt active power filter with battery interface for uninterruptible power supply (UPS) operation. The proposed unified architecture is composed by a single-phase ac-dc converter from the power grid side and by a bidirectional isolated dc-dc converter to interface the batteries, allowing the operation in three distinct modes: (1) Shunt active power filter; (2) Off-line UPS to supply a set of priority loads during power outages; (3) Energy storage system to support the power grid. The proposed architecture and the developed control algorithms were validated with a reduced-scale laboratorial prototype in all the three different operation modes. The presented experimental results highlight the benefits of the proposed architecture.**

Index Terms—**Active Power Filter, Uninterruptible Power Supply, Bidirectional Isolated dc-dc Converter, Power Quality.**

I. INTRODUCTION

Nowadays, electrical energy is indispensable to the comfort and needs of society. However, due to the everlasting utilisation of nonlinear loads, harmonic currents flow in the power grid, polluting it [1]. Once power quality problems lead to financial costs, it is of utmost importance to mitigate these power quality issues [2]. A shunt active power filter (SAPF), whose concept was proposed in 1971 [3], is a power electronics based equipment capable of mitigating harmonic currents and compensating power factor of a set of loads connected to the power grid [4]. A line-commutated SAPF for fundamental reactive power compensation was made practicable in [5], and a full-controlled SAPF also allowing harmonic currents compensation was proposed in [6]. A SAPF is comprised by an ac-dc bidirectional converter connected in parallel with the power grid, providing the harmonic currents and reactive power consumed by the loads, allowing the power grid to supply only active power, i.e., a sinusoidal current in phase with the power grid voltage. Over the last decades, extensive research has been made in terms of new compensation capabilities, topologies and control schemes for SAPFs. A

Tiago J. C. Sousa is with Centro Algoritmi, University of Minho, Campus of Azurem, Guimaraes, 4800-058, Portugal (e-mail: a61909@alunos.uminho.pt)

Jose A. Afonso is with CMEMS-UMinho, University of Minho, Campus of Azurem, Guimaraes, 4800-058, Portugal (phone: 351-253510190; fax: 351-253510189; e-mail: jose.afonso@dei.uminho.pt).

Vítor Monteiro, J. G. Pinto and João L. Afonso are with Centro Algoritmi, University of Minho, Campus of Azurém, Guimarães, 4800-058, Portugal (e-mail: {vmonteiro, gpinto, jla}@dei.uminho.pt).

widespread review about SAPF for power quality improvement is presented in [7].

Besides problems associated with currents, there are power systems where it is mandatory to incessantly provide power to specific loads. In industries, power outages can be reflected in production failure, which carries large financial costs. In [8] are presented some examples about how power outages inflict costs in sectors like financial trading, computer centres and telecommunications. Unpredicted power outages can be mainly triggered by natural catastrophes, e.g., lightning strikes and earthquakes, and can last for minutes or even days. In medical facilities, power outages can be hazardous to human life, causing respiratory issues, inability to sterilize instruments, processing X-rays and to properly transport patients between floors due to unavailable elevators [9]. Towards the referred consequences, it is crucial for a power system to be prepared for power outages, requiring the utilisation of an energy backup. An uninterruptible power supply (UPS) allows a ceaselessly deliver of electrical power for a set of priority loads. Several UPS topologies have been developed with different protection levels, as well as efficiency and cost related diversity [10].

Analysing a SAPF and an off-line UPS system from the power grid point of view, it is possible to identify that the power converter of both systems is very similar, comprising a parallel grid-connected ac-dc converter [11]. However, an off-line UPS has an additional converter to charge the batteries. Therefore, connecting a dc-dc converter to the dc side of the SAPF, it is possible to endow the SAPF with the features of an off-line UPS. In [12] is proposed an off-line UPS with active filtering capabilities using a high-frequency transformer and a cycloconverter. However, it requires four bidirectional cells, each one being comprised by several power semiconductors, leading to higher conduction losses. In [13] is presented a modular UPS system with active filtering capabilities, but the SAPF and the modular UPS consist of different power converters. The combined operation of SAPF and UPS is studied in [14] for a three-phase system, however, using a non-isolated dc-dc converter, requiring a large battery pack for grid connected applications.

In this context, this paper proposes a single-phase unified architecture of a SAPF with battery interface for UPS operation, i.e., with an energy storage interface. The proposed architecture is composed by an ac-dc converter connected in parallel with the power grid (i.e., similarly to a traditional SAPF), and by a bidirectional isolated dc-dc converter (i.e., similarly to the dc-dc converter of an off-line UPS). The ac-dc converter can operate as a SAPF producing
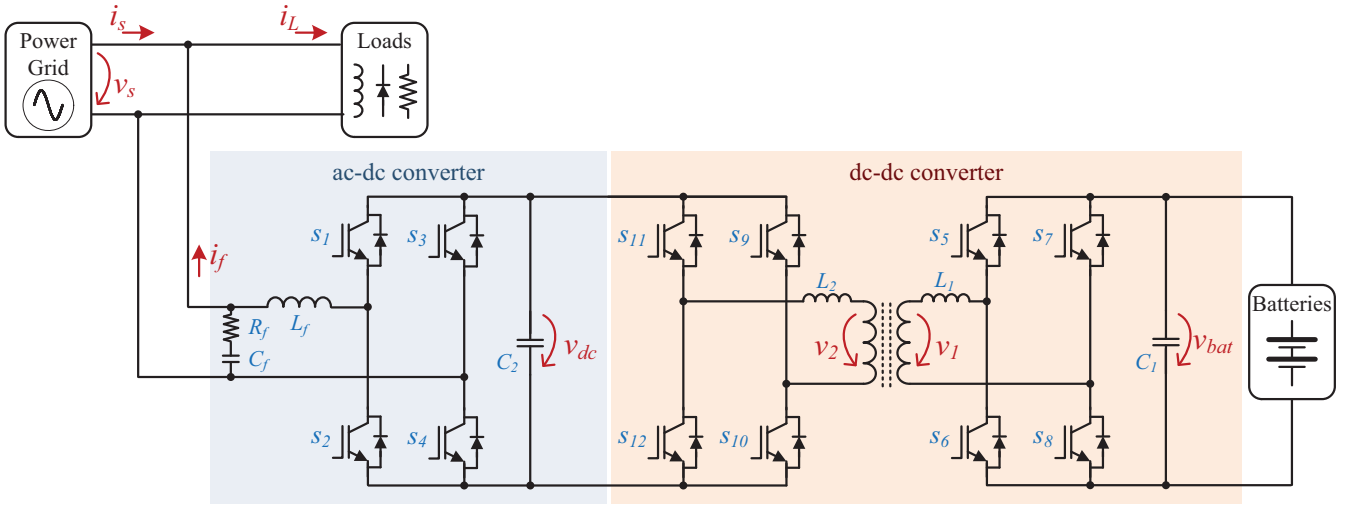
Fig. 1. Electrical circuit of the unified architecture of active power filter with energy storage interface.

the harmonic currents and reactive power required by the loads and charging the batteries at the same time, or as UPS producing a sinusoidal voltage to feed the loads. On the other hand, the bidirectional isolated dc-dc converter can be controlled to charge the batteries (with constant voltage and constant current) or discharge the batteries during the operation as an off-line UPS. It is important to note that the operation as off-line UPS only occurs during power outages, i.e., the control algorithm identifies the power outage and changes the control algorithm for such operation mode. Moreover, once the dc-dc converter is isolated, it is possible to use a smaller battery pack, since a higher conversion ratio can be achieved with a high-frequency transformer compared to non-isolated topologies, representing an important contribution of the proposed architecture.

II. Principle of Operation

This section presents the principle of operation of the proposed unified architecture of SAPF with battery interface for UPS operation. Fig. 1 shows the electrical circuit of the unified architecture. As it can be seen it is composed by two power converters: a bidirectional ac-dc converter to interface the power grid, and a bidirectional isolated dc-dc converter to interface the batteries. These two converters are analysed in detail along this section.

A. Ac-dc Converter

The ac-dc converter is a full-bridge topology composed by two legs. This converter is used during all the three different operation modes. During the operation as SAPF it is controlled as a current source to control the grid current. The reference for the grid current is obtained with the Fryze-Buchholz-Depenbrock (FBD) power theory proposed in [15][16]. With this theory it is calculated the active power consumed by the loads in order to determine the in-phase, fundamental current desirable to be provided by the power grid. Thus, the SAPF must supply the harmonic content and reactive power demanded by the loads. The reference current for the SAPF (i_f^*) is obtained according to:

$$i_f^* = i_L - \frac{P v_s}{V_S^2}, \qquad (1)$$

where i_L is the load current, P is the active power consumed by the loads, v_s is the power grid voltage, and V_s^2 is the squared rms power grid voltage. It is important to note that, in the presence of a distorted power grid voltage, the grid current will also be distorted. Sinusoidal grid current can be obtained using a slight modification in the presented control theory, which consists in using the fundamental component of the power grid voltage instead of the measured ones. The fundamental component of the power grid voltage can be determined by means of a phase-locked loop (PLL) algorithm. The current produced by the SAPF is controlled by means of a PI. The dc-link voltage is controlled according to its reference also using a PI controller to generate the regulation power (p_{reg}). This variable represents an additional power component that must be provided by the power grid to control the voltage across the dc-link capacitors. Therefore, P is replaced by $P + p_{reg}$ in order to determine the SAPF reference current. Besides the operation as SAPF, during this operation mode the ac-dc converter can also be used to transfer energy from the power grid to charge the batteries through the bidirectional isolated dc-dc converter. Therefore, another power component is added to the SAPF reference current, according to:

$$i_f^* = i_L - \frac{(P + p_{reg} + p_{bat})}{V_S^2} v_{spll}, \qquad (2)$$

where v_{spll} is the fundamental component of the power grid voltage obtained by means of a PLL, and p_{bat} is equal to the product of batteries current and batteries voltage, meaning the additional power demanded by the SAPF in order to charge the batteries with the desired current and voltage.

During the operation as UPS, the ac-dc converter is controlled as a voltage source to obtain a sinusoidal output voltage to feed the loads during the power outages. The reference voltage is obtained with the PLL algorithm. The output voltage is controlled using a dual-loop PI controller, where are used the voltage produced by the converter, the current consumed by the loads (which is the same as the converter output current) and its derivative.

The output reference voltage of the converter (v_{fref}) is obtained according to:

$$v_{fref}[k] = k_{pv} v_{err}[k] + k_{iv} v_{sum\_err}[k] + \\ + k_{pi} i_f[k] + k_{di} \Delta i_f[k] , \qquad (3)$$

where v_{err} is the output voltage error, v_{sumerr} is the output voltage error sum, i_f is the output current, T_s is the sampling period and k_{xx} are controller gains, where the first index (p, i or d) means the controller component (proportional, integral or derivative) and the second index (v or i) represents voltage or current quantities. The output current derivative Δi_f is determined according to:

$$\Delta i_f[k] = \frac{i_f[k] - i_f[k-1]}{T_S}. \qquad (4)$$

In the scope of this paper, it was used a PI controller for the output voltage and a proportional-derivative (PD) controller for the output current in order to achieve a suitable performance in the presence of nonlinear loads.

B. Bidirectional Isolated dc-dc Converter

The dc-dc converter consists in a voltage-fed dual-active-bridge topology, where the primary side is the low-voltage side and is connected to the batteries and the secondary side is the high-voltage side, sharing the dc-link with the ac-dc converter. Both sides are connected by a high-frequency transformer, allowing isolation and a high voltage conversion ratio.

The dual-active-bridge topology can be operated using modulation techniques like pulse-width modulation (PWM), phase shift and deviations from the latter. Phase shift [17] allows a flexible power transfer between both sides of the converter, being one of the most popular modulation techniques applied to isolated dc-dc converters, such the presented topology. Each side of the converter produces a 50% duty-cycle square-wave, being applied a phase shift between both voltages. The applied phase angle has direct impact in the transferred power, with the latter increasing with the phase shift. Besides, phase shift modulation allows active rectification, as opposed to PWM, where one converter side is switched at each time. When low voltage values are involved, the latter brings a reduced efficiency due to the voltage drops on the output antiparallel diodes [18]. Despite the aforementioned advantages, however, phase shift modulation is not suitable when the voltages applied to the transformer windings are discrepant with respect to transformer turns ratio. This situation leads to substantial currents in the transformer, as well as in the power switches, even if the transferred power is low. Thus, the converter operates with high values of reactive power. To overcome this issue, variants of the phase shift modulation technique were developed, e.g., dual phase shift [19] and triple phase shift [20]. These modulation techniques apply, respectively, two or three distinct phase angles to the converter, using a phase difference between two legs of the same bridge. Thus, circulating currents and consequently reactive power can be reduced using these modulation techniques. In addition, both PWM and phase shift modulation techniques can be combined in order to reduce the reactive power involved [21]. Therefore, a phase shift modulation technique combined with duty-cycle control was implemented for power transfer, reducing the current stress in the switches and transformer windings. The duty-cycle value is obtained with a PI controller, generating high values of duty-cycle when the dc side converter voltages have a close relationship in respect with the transformer turns ratio and low values of duty-cycle for the opposite case. The phase angle is obtained also by means of a PI controller and is responsible for dc-link voltage regulation when the system is operating in UPS mode and controls the charging of the batteries when the system operates as SAPF.

III. Developed Prototype

This section shows in detail the developed laboratorial prototype, mainly focusing the digital control structure and the hardware power structure. Fig. 2 shows the laboratorial workbench, including the developed prototype, and Table I presents the main parameters of this prototype.

A. Control Structure

In order to control the aforementioned power converters it was used a digital control structure. The main core of such structure is the digital signal processor (DSP) model TMS320F28377S from Texas Instruments, where are implemented the digital control algorithms. This DSP has incorporated an internal ADC with 14 channels and with 12 bits of resolution, as well as an internal DAC with 8 channels and with 12 bits of resolution, and several PWM output channels. The voltages and currents are acquired with the CYHVS5-25A and HAIS 50-P hall-effect sensors. The output signals of such sensors are bipolar and in current, therefore, it is used a signal conditioning circuit to converter the current signals to voltage signals, as well to adapt the voltage range of each signal to the unipolar voltage of the ADCs channels. The signal conditioning is processed using a summing amplifier circuit. The output control signals from the DSP are processed by a command circuit with the intent to convert the 3 V transistor-transistor logic (TTL) signals of the DSP to 15 V complementary metal-oxide-semiconductor (CMOS) logic signals. In this command circuit it is also used a protection circuit, which is activated from the signal conditioning circuit, i.e., if some of the voltages or currents exceeds a nominal predefined value, then an error is deployed to control the command circuit. The output signals from the command circuit are then used as input for the IGBT and MOSFET gate driver circuits. These gate drivers are based in the ADUM3223 from Analog Devices. In the scope of this project were used 6 driver circuits, once each one is able to control two power semiconductors.

B. Power Structure

As described in section II, the power structure is divided in two main converters, the ac-dc and the bidirectional isolated dc-dc. These converters are described as follows.

1) Ac-dc Converter

The ac-dc converter is a full-bridge converter and is composed by four IGBTs model IKW40N65F5 from Infineon Technologies (maximum collector-emitter voltage of 650 V and maximum collector current of 40 A). In the scope of this project, these IGBTs are switched at 50 kHz, In order to prevent malfunctions it is used a protection circuit for the gate, i.e., a circuit between the driver and the gate and emitter terminals of the IGBT. In order to couple the ac-dc converter with the power grid it is used an inductor with nominal inductance of 1.2 mH and nominal current of 20 A. Additionally to this inductor it is used a RC passive
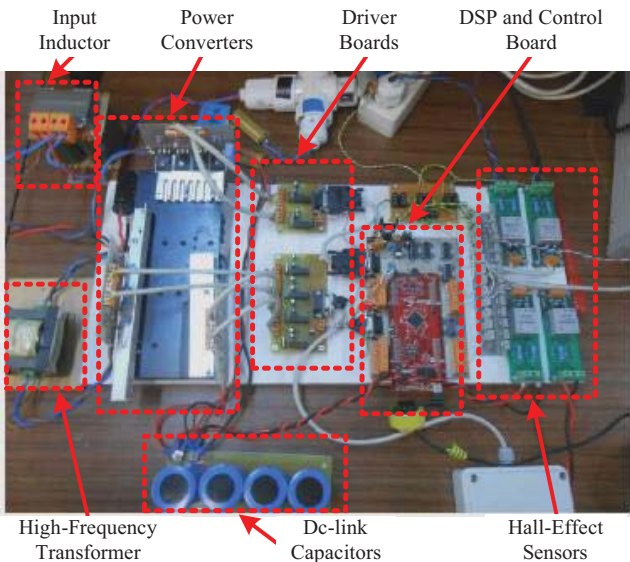
Fig. 2. Laboratorial workbench with the developed prototype.

Table I. Main parameters of the developed prototype.

Parameter	Value
Power Grid Voltage	230 V
Power Grid Frequency	50 Hz
Maximum Grid Current	16 A
Dc-link Voltage	400 V
Switching Frequency (ac-dc)	50 kHz
Switching Frequency (dc-dc)	100 kHz
High-Frequency Transformer Ratio	1:15
Maximum Power as UPS	1 kW
Batteries Voltage	23 V to 29 V
Batteries Current	40 A

filter with a capacitance of 10 µF and resistance of 8 Ω. The 8 Ω resistor is applied with the purpose of damp possible resonances between the capacitive and inductive elements of the passive filter. For the dc-link are used four capacitors model MAL209527821E3 from Vishay in order to perform a nominal capacitance of 3.28 mF with a maximum voltage of 450 V.

2) Bidirectional Isolated dc-dc Converter

The dc-dc converter is a dual-active-bridge dc-dc converter composed by four MOSFETs model PSMN015-60PS from NXP Semiconductor (maximum drain-source voltage of 60 V, maximum drain current of 50 A, and drain-source on-resistance of 14.8 mΩ) and four MOSFETs model IPP50R500CE from Infineon Technologies (maximum drain-source voltage of 500 V, maximum drain current of 11 A and drain-source on-resistance of 500 mΩ). In the scope of this project, these MOSFETs are switched at 100 kHz, and, similarly to the IGBTs of the ac-dc converter, it is used a protection circuit for the gate, i.e., a circuit between the driver and the gate and source terminals of the semiconductor. In the batteries side it is used a capacitor with nominal capacitance of 4.7 mF and nominal voltage of 63 V. The galvanic isolation between the primary and secondary converters is performed using a 1:15 high-frequency transformer specially developed for this project using ferrites model B66397G0000X187 from Epcos. The primary nominal current is 45 A (were

used 59 AWG25 wires in parallel) and the secondary nominal current is 3 A (were used 3 AWG23 wires in parallel).

IV. EXPERIMENTAL VALIDATION

This section presents the main experimental results obtained to prove the proper operation of the proposed unified architecture and to highlight its main benefits. Therefore, this section is divided in three distinct modes of operation: SAPF; UPS; and energy storage system.

A. Operation as SAPF

This item presents the operation of the proposed unified architecture during the operation as SAPF. The first process of this operation mode is the synchronization with the fundamental component of the power grid voltage, where is used the phase-locked loop (PLL) algorithm proposed in [22]. After that, considering the current consumed by the loads connected in the same electrical installation, it is determined the reference current that the converter must produce in order to obtain a sinusoidal grid current. The details about the determination of the grid reference current are presented in section II (a).

Fig. 3 shows the experimental results obtained with the developed laboratory prototype during the operation as SAPF. In this figure it is possible to see the power grid voltage (v_s), the load current (i_L), which is the grid current (i_s), the dc-link voltage (v_{dc}), and the converter current reference (i_c^*) calculated by the DSP. From this figure it is possible to see that the current consumed by the loads (i_L) has a high harmonic distortion and, consequently, to cancel such harmonic distortion, the determined converter current reference (i_c^*) has also a high harmonic distortion. In this experimental result, it is important to note that the dc-link voltage is not yet controlled to its reference, i.e., the converter only determines the reference current and is not yet compensating the currents.

Fig. 4 shows the power grid voltage (v_s), the grid current (i_s), and the dc-link voltage (v_{dc}) during the operation as SAPF. As it can be seen, due to this operation mode, the grid current (i_s) is sinusoidal with reduced harmonic distortion (THD% = 3.6%), and in phase with the power grid voltage (v_s), i.e., from power grid point of view, the electrical installation only operates with fundamental active power. It is also important to note that the dc-link voltage is regulated to the reference value, maintaining a proper value in order to allow the accurate operation of the SAPF.

B. Operation as UPS

This item presents the operation of the proposed unified architecture during the operation as UPS. This operation mode only occurs during power outages, when control changes, so that the ac-dc converter stops operating as SAPF, and begins to produce a sinusoidal voltage to feed the electrical loads. Therefore, the first algorithm is the detection of power outages. For such purpose it was used the half-cycle rms value of the power grid voltage to detect when it falls below a threshold of 10% of the nominal value. Fig. 5 shows the power grid voltage (v_s), the rms value of the power grid voltage (V_s) and a flag used to indicate when
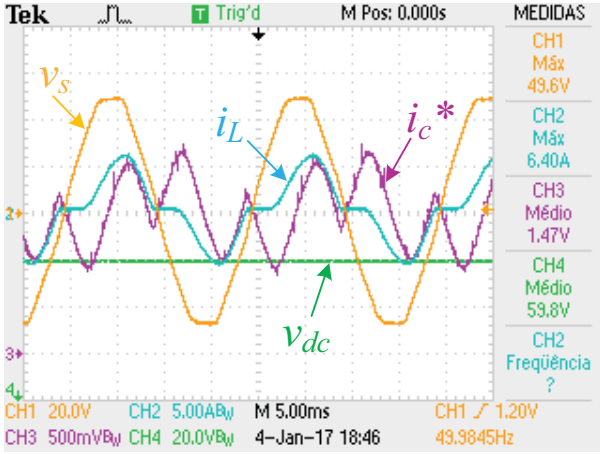
Fig. 3. Experimental results during the operation as active power filter: Power grid voltage (v_s); Load current (i_L); Dc-link voltage (v_{dc}); Converter current reference (i_c^*).
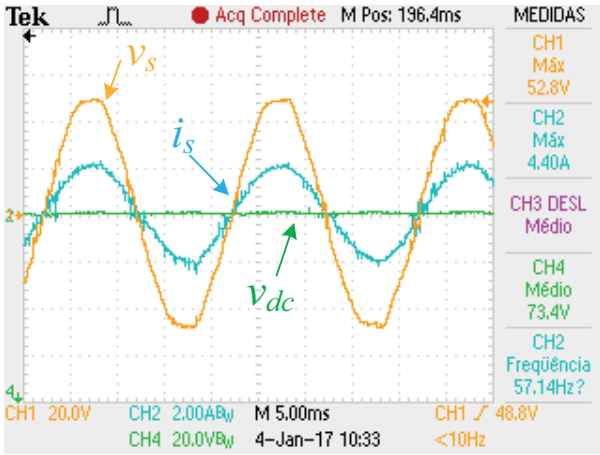

Fig. 5. Experimental results during the operation as UPS: Power grid voltage (v_s); Rms value of the power grid voltage (V_s); Flag used to indicate a power outage (*outage*).

Fig. 4. Experimental results during the operation as active power filter: Power grid voltage (v_s); Grid current (i_s); Dc-link voltage (v_{dc}).

Fig. 6. Experimental results during the operation as UPS: Converter output voltage (v_f); Load current (i_f); Dc-link voltage (v_{dc}).

a power outage is detected. As it can be seen, a power outage occurs during the positive half-cycle approximately at 30^0, and the DSP takes approximately 2 milliseconds to identify the power outage. As aforementioned, when a power outage occurs, the control algorithm is changed to the ac-dc converter produce a voltage. Fig. 6 shows the power grid voltage (v_s) and the current consumed by the loads (i_f) during the operation as UPS. As it can be seen, due to the control algorithm used by the ac-dc converter during this operation mode, the voltage produced is sinusoidal even with a distorted current consumption, representing an added value of the proposed unified architecture.

Besides the ac-dc converter, during this operation mode, it is necessary to use the bidirectional isolated dc-dc converter. Therefore, Fig. 7 shows the voltage applied to the primary winding of the isolated transformer (v_1), the voltage applied to the secondary winding of the isolated transformer (v_2), the current in the primary winding (i_1), and the dc-link voltage (v_{dc}). As expected, due to the control algorithm (described in section II), the voltage in the secondary winding is not in phase with the voltage in the primary winding to enable the power transfer.

C. Operation as Energy Storage System

This item presents the operation of the proposed unified architecture during the operation as energy storage system, i.e., when both ac-dc and dc-dc converter are used to charge the batteries. It is important to note that this operation mode
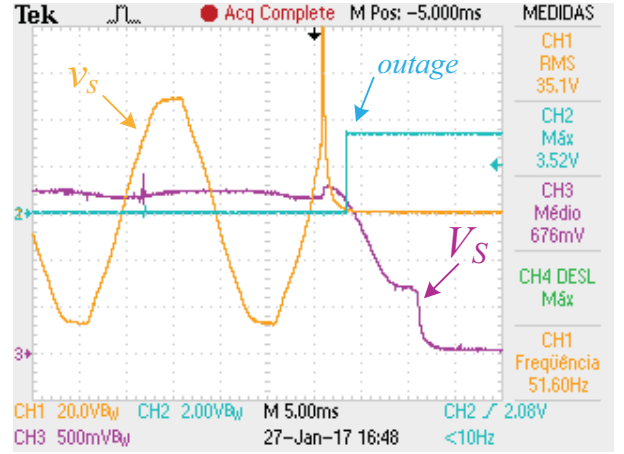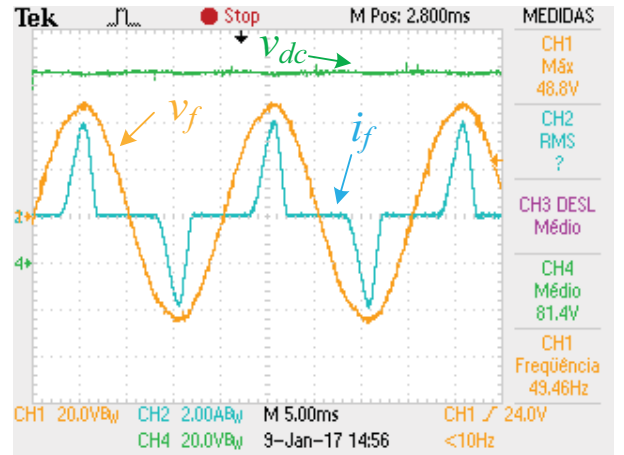
can be performed with the ac-dc converter operating as SAPF. The energy stored in the batteries can be used in two distinct scenarios: (1) It can be injected into the power grid during the operation of the ac-dc converter as SAPF; (2) It can be used to feed the electrical loads during power outages, i.e., during the operation as UPS. The main experimental results of the operation of both ac-dc and dc-dc converters in these scenarios were presented in the previous items. Nevertheless, taking into account the importance of the isolation transformer, Fig. 8 shows the voltage in the primary winding of the transformer (v_1), the voltage in the secondary winding of the transformer (v_2), the current in the primary winding (i_1), and the batteries voltage (v_{bat}). As it can be seen, in Fig. 7 the primary winding voltage of the high-frequency transformer leads the secondary winding voltage (i.e., the energy flows from the batteries to the dc-link), and in Fig. 8 the primary winding voltage lags the secondary winding voltage (i.e., the energy flows from the dc-link to the batteries).

V. CONCLUSION

This paper presented a unified architecture of single-phase shunt active power filter with battery interface for uninterruptible power supply (UPS) operation. Along the paper is introduced the principle of operation and is performed a detailed description of the developed control and power circuits including the applied control algorithms.
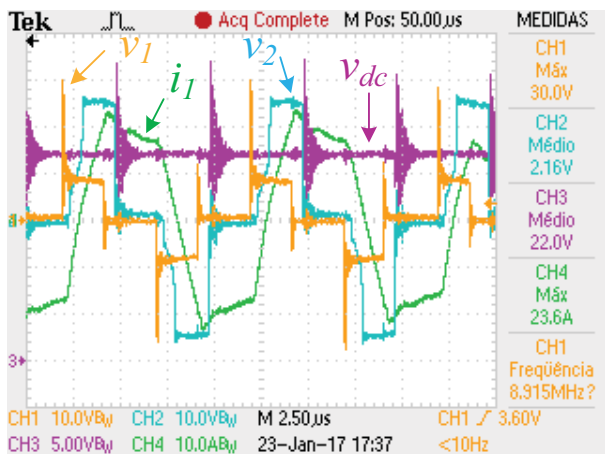
Fig. 7. Experimental results during the operation as UPS: Voltage in the primary winding of the transformer (v_1); Voltage in the secondary winding of the transformer (v_2); Current in the primary winding (i_1); Dc-link voltage (v_{dc}).
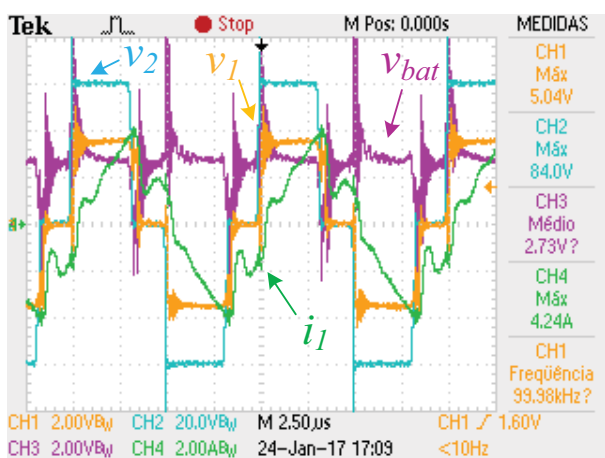

Fig. 8. Experimental results during the operation as energy storage system: Voltage in the primary winding of the transformer (v_1); Voltage in the secondary winding of the transformer (v_2); Current in the primary winding (i_1); Batteries voltage (v_{bat}).

The experimental results were obtained to validate the proposed integrated architecture and the control algorithms through three distinct modes of operation: (1) Shunt active power filter; (2) Isolated UPS to supply a set of priority loads during power outages; (3) Energy storage system to support the power grid. The proposed system can be an optimal solution for single-phase installations, allowing the compensation of power quality problems related with current harmonics, power factor and power outages.

REFERENCES

[1] A. Araújo, J. G. Pinto, B. Exposto, C. Couto, and J. L. Afonso, "Implementation and Comparison of Different Switching Techniques for Shunt Active Power Filters," IEEE IECON Industrial Electronics Society Conference, pp.1519-1525, Nov. 2014.

[2] Roger C. Dugan, Mark F. McGranaghan, S. Santoso, H. W. Beaty, "Electrical Power Systems Quality," McGraw-Hill (3rd Edition), pp. 373–435, 2002.

[3] H. Sasaki, T. Machida, "A new method to eliminate ac harmonic currents by magnetic flux compensation - considerations on basic design," IEEE Trans. Power App. Syst., vol.PAS-90, no.5, pp.2009-2019, 1971.

[4] J. G. Pinto, Bruno Exposto, Vitor Monteiro, L. F. C. Monteiro, Carlos Couto, João L. Afonso, "Comparison of Current-Source and Voltage-Source Shunt Active Power Filters for Harmonic Compensation and Reactive Power Control," IEEE IECON Industrial Electronics Society Conference, pp.5124-5129, Oct. 2012.

[5] L. Gyugyi, E. C. Strycula, "Active AC Power Filters," IEEE IAS Industry Applications Society Annual Meeting, pp.529-535, 1976.

[6] H. Akagi, Y. Kanazawa, A. Nabae, "Instantaneous Reactive Power Compensators Comprising Switching Devices without Energy Storage Components," IEEE Trans. Ind. Appl., vol.IA-20, no.3, pp.625–630, May 1984.

[7] B. Singh, K. Al-Haddad, and A. Chandra, "A Review of active filters for power quality improvement," IEEE Trans. on Ind. Electron., vol.46, no.5, pp.960–971, Oct. 1999.

[8] Neil Hodge, "Energy Risks - the dangers of power cuts and blackouts," Emerging Risks (Allianz), pp.28-33, 2015.

[9] Healthcare & Public Health Sector Coordinating Councils, "Planning for Power Outages: A Guide for Hospitals and Healthcare Facilities," 2003.

[10] J. P. Beaudet, J. N. Fiorina, and O. Pinon, "UPS topologies and standards," MGE-UPS Systems, 1999.

[11] A. Emadi, A. Nasiri, and S. B. Bekiarov, Uninterruptible Power Supplies and Active Filters. CRC Press, 2005.

[12] V. John and N. Mohan, "Standby power supply with high frequency isolation," IEEE APEC Applied Power Electronics Conference and Exposition, pp.990–994, Mar. 1995.

[13] Chi Zhang, Josep M. Guerrero, Juan C. Vasquez, "A simplified control architecture for three-phase inverters in modular UPS application with shunt active power filter embedded," ECCE International Conference on Power Electronics, pp.413–420, June 2015.

[14] Bruno Exposto, J. G. Pinto, H. Goncalves, Vitor Monteiro, D. Pedrosa, C. Couto, J. L. Afonso, "Evaluation of a Shunt Active Power Filter with energy backup capability," IEEE IECON Industrial Electronics Conference, pp.5963–5968, Nov. 2013.

[15] M. Depenbrock, "The FBD-method, a generally applicable tool for analyzing power relations," IEEE Trans. Power Syst., vol.8, no.2, pp.381–387, May 1993.

[16] Telmo Santos, J. G. Pinto, P. Neves, D. Gonçalves, João L. Afonso, "Comparison of Three Control Theories for Single-Phase Active Power Filters," IEEE IECON Industrial Electronics Society Conference, Nov. 2009.

[17] R. W. A. A. De Doncker, D. M. Divan, M. H. Kheraluwala, "A Three-Phase Soft-Switched High-Power-Density DC/DC Converter for High-Power Applications," IEEE Trans. Ind. Appl., vol.27, no.1, pp.63–73, Jan. 1991.

[18] J. Sebastian, J. A. Cobos, O. Garcia, J. Uceda, "An overall study of the half-bridge complementary-control DC-to-DC converter," IEEE PESC Power Electronics Specialist Conference, vol.2, pp.1229-1235, June 1995.

[19] Hua Bai, Chris Mi, "Eliminate Reactive Power and Increase System Efficiency of Isolated Bidirectional Dual-Active-Bridge DC–DC Converters Using Novel Dual-Phase-Shift Control," IEEE Trans. Power Electron., vol.23, no.6, pp.2905–2914, Dec. 2008.

[20] Kuiyuan Wu, Clarence W. de Silva, William G. Dunford, "Stability analysis of isolated bidirectional dual active full-bridge DC-DC converter with triple phase-shift control," IEEE Trans. Power Electron., vol.27, no.4, pp.2007–2017, Apr. 2012.

[21] Dehong Xu, Chuanhong Zhao, Haifeng Fan, "A PWM plus phase-shift control bidirectional dc-dc converter," IEEE Trans. Power Electron., vol.19, no.3, pp.666–675, May 2004.

[22] M. Karimi-Ghartemani, M. R. Iravani, "A new phase-locked loop (PLL) system," IEEE MWSCAS Midwest Symposium on Circuits and Systems, vol.1, pp.421–424, Aug. 2001.